The photoelectron spectroscopy of the dichloroethylenes: the geminal isomer 1,1-$Cl_2C_2H_2$. An experimental and quantum chemical study

Journal of Physics Communications

OPEN ACCESS

RECEIVED
9 June 2017

REVISED
15 September 2017

ACCEPTED FOR PUBLICATION
5 October 2017

PUBLISHED
27 December 2017

PAPER

The photoelectron spectroscopy of the dichloroethylenes: the geminal isomer 1,1-$Cl_2C_2H_2$. An experimental and quantum chemical study

R Locht[1], D Dehareng[2] and B Leyh[1]

[1] Laboratory for Molecular Dynamics, Department of Chemistry, Institute of Chemistry, Bât.B6c, University of Liège, Sart-Tilman B-4000 Liège 1, Belgium

[2] Centre d'Ingéniérie des Protéines, Institute of Chemistry, Bât.B6a, University of Liège, Sart-Tilman B-4000 Liège 1, Belgium

E-mail: robert.locht@ulg.ac.be

Keywords: photoelectron spectroscopy, synchrotron radiation, quantum chemical calculations, 1,1-$Cl_2C_2H_2$, constant ion state spectroscopy, electronic states, vibrational structure

Supplementary material for this article is available online

Abstract

This work analyzes the threshold photoelectron spectrum (TPES) and selected constant ion state (CIS) spectra of the 1,1-$C_2H_2Cl_2$ isomer measured using synchrotron radiation. The TPES is compared to the HeI-, NeI- and ArII-photoelectron spectra (PES). In the HeI-PES nine photoelectron bands have been observed at vertical ionization energies of 9.992 eV, 11.652 eV, 12.157 eV, 12.536 eV, 13.633 eV, 14.195 eV, at about 15.9 eV and 16.2 eV and at 18.496 eV successively. For most of these bands the adiabatic ionization energy could be determined and a detailed vibrational analysis of the first four bands is presented. All these bands exhibit an extended vibrational structure. In particular, the ground electronic state and the third excited state display an extended vibrational structure upon excitation by the ArII-resonance line. The assignments of the electronic bands and of the vibrational structure are based on quantum chemical calculations. These allowed us to assign the nine electronic states in terms of ionization and double excitation in a molecular orbital scheme. The good correlation between predicted vibrational wavenumbers and the experimental values allowed us to assign all observed vibrational structures. The CIS spectrum of the eight first electronic states of 1, 1-$C_2H_2Cl_2^+$ have also been recorded. Vibrationally resolved CIS spectra of the molecular ion ground state have been obtained and are discussed.

1. Introduction

We recently reported a detailed investigation of the vacuum UV photoabsorption spectrum (PAS) and the photoelectron spectroscopy (PES) of the disubstituted halogenated ethylenes, i.e. 1,1-$C_2H_2F_2$, 1,1-C_2H_2FCl and cis- and trans-1,2-C_2H_2FCl [1]. Quantum chemical calculations were performed to support the interpretation and assignments of the successive electronic bands with their associated vibrational structure.

In contrast to these compounds, spectroscopic investigations devoted to the three isomers of dichloroethylene have received much more attention in the literature. This is likely linked to the broader field of chemical and industrial applications as well as to the environmental impact of these molecular species.

The HeI-PES of the geminal 1,1-$C_2H_2Cl_2$ isomer has been reported several times in the early 70s [2–4]. The only HeII (30.4 nm) spectrum of this molecule has been published by Von Niessen *et al* [5] who interpreted the spectrum and assigned the numerous bands based on quantum chemical calculations.

More recently, Parkes *et al* [6] published the threshold photoelectron spectrum (TPES) of the three isomers of $C_2H_2Cl_2$ by using dispersed synchrotron radiation. These authors used the threshold photoelectron-photoion coincidence technique to investigate the dissociative photoionization dynamics of these molecules. Quantum chemical calculations at different levels were applied to assign the photoelectron bands.

At about the same time Zhou *et al* [7] measured the infrared spectra of the dichloroethylene molecular ions trapped in a solid Argon matrix at 4 K. The 1,1 -$C_2H_2Cl_2^+$ and trans-1,2-$C_2H_2Cl_2^+$ IR spectra have been reported. These authors also assigned the spectral patterns based on quantum chemical wavenumber calculations.

In an ongoing work on 1,1-$C_2H_2Cl_2$, its vacuum UV PAS [8] and photoelectron spectrum have been remeasured. These data are complemented by the measurements of the NeI- and ArII-PES. The TPES at improved resolution and constant ion state (CIS) spectra have been recorded using synchrotron radiation. *Ab initio* quantum chemical calculations have been performed to assign the electronic bands and identify the individual vibrational wavenumbers of the cation in their ground electronic state as well as in several excited states. The present paper focuses on the photoelectron, TPES and CIS spectroscopy.

2. Experimental

2.1. Experimental setups

The two experimental setups used in this work have been described in detail in [9, 10]. The most relevant information is reproduced here.

The fixed-wavelength photoelectron spectrometer used in this work is part of a PEPICO experiment [9] equipped with an effusive gas inlet. The VUV light produced by a discharge in He (58.43 nm or 21.22 eV), Ne (73.58–74.37 nm or 16.850–16.671 eV) or ArI (104.82–106.67 nm or 11.828–11.623 eV)-ArII (91.97 nm or 13.480 eV), is introduced in the ion chamber through a capillary of 0.5 mm diameter. A photoelectric light detector (a gold diode) continuously monitors the light source. Photoelectrons are extracted in the opposite direction to the ions and transmitted through a retarding potential analyzer with a differential output [11]. The photoelectron energy resolution, obtained under coincidence conditions, is 30 meV as measured on Ar^+/e^- coincidence data.

The TPES and CIS spectroscopy experimental setup uses the synchrotron radiation available from the BESSY facility (Berlin, Germany). It was dispersed by a 3m-NIM monochromator equipped with a platinum-grating of 2400 lines mm^{-1} with maximum transmission in the 10–40 eV (124–31 nm) range. An adequate signal-to-noise ratio is reached by adjusting the entrance and exit slits between 100 and 200 μm.

The light beam is focused into an ion chamber, in the focussing plane of a tandem electron spectrometer consisting of two 180° electrostatic deflectors [10]. Under constant pass energy (E_0) conditions, the full width at half-maximum energy resolution (ΔE) remains constant and is given by $\Delta E/E_0 = w/104$, where w is the slit width (in millimeters). In the present work, $w = 0.5$ or 1.0 mm while E_0 is chosen between 1.0 and 10.0 V to obtain a sufficient signal for each type of experiment.

The TPES operating mode corresponds to 'constant photoelectron energy' spectroscopy. The electron accelerating voltage V_{acc} is kept as close as possible to E_0, transmitting only TPE. A global photoelectron energy resolution of 5 meV is achieved.

In a CIS spectroscopy experiment, the relative partial ionization cross sections of well-defined electronic/vibrational states of the molecular ion are measured as a function of the incident photon energy $h\nu$. $h\nu$ and the electron kinetic energy $E_{kin}{}^e$ have to be scanned in parallel to keep the difference $IE_{E,\nu} = h\nu - E_{kin}{}^e$ constant where $IE_{E,\nu}$ corresponds to the ionization energy of the selected electronic/vibrational ionic state.

Both the TPES and CIS spectra have to be corrected for (i) the decreasing synchrotron storage ring beam current and (ii) the monochromator transmission function measured by the photoelectron signal of a gold diode, positioned in the ion chamber at the opposite of the monochromator exit slit. In addition, the CIS spectrum has to be corrected for the electron energy analyzer transmission function. For this purpose, the CIS curve of $Xe^+(^2P_{1/2})$ is recorded and assimilated to the transmission function. This curve is structureless indeed over a broad energy range except for weak autoionization resonances assigned to the Rydberg $Xe(^1S_0) \rightarrow Xe(^2S_{1/2})6p$ transition [12] at about 7.5 eV above threshold. Through the normalization process, they bring about an undesired but well-identified contamination of the CIS data in a range where the dichloroethylene ionization cross section is usually flat. No attempt has been made to remove these extremely weak structures. In practice the CIS spectra are just analyzed with an awareness of this contamination.

1,1-$C_2H_2Cl_2$, (ABCR, 98% purity) has been used without further purification.

2.2. Data handling and error estimation

To facilitate the characterization of weak sharp peaks superimposed on an intense continuum, a continuum subtraction procedure developed by Carbonneau *et al* [13, 14] has been applied. This method has proved successful in other spectral analyses [1, 14–17]. In practice, we first simulate the underlying continuum by a severe smoothing of the experimental spectrum. Upon subtraction of this continuum from the original data, we obtain a spectral curve called Δ-plot.

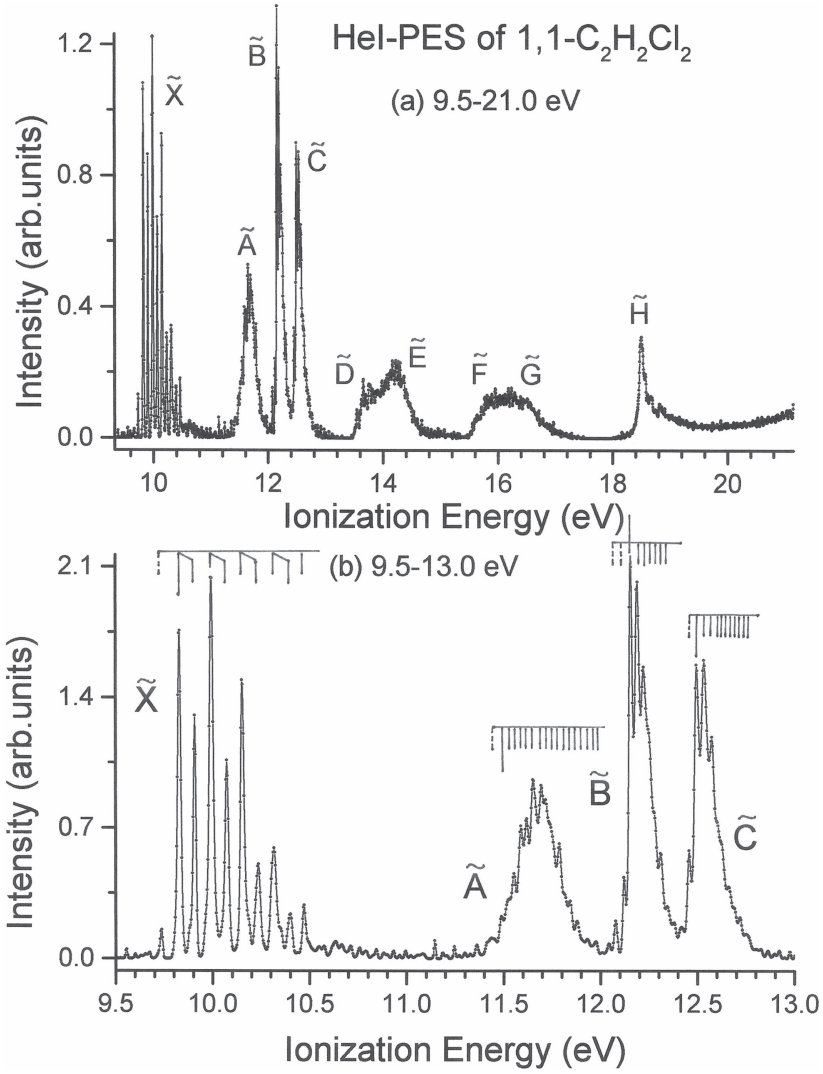

Figure 1. HeI- photoelectron spectrum (PES) of 1,1-$C_2H_2Cl_2$ between (a) 9.5 and 21 eV, and (b) 9.5 and 13.0 eV. Vertical bars show the vibrational structure. Only the two highest wavenumbers are represented for the $\tilde{X}^2B_1$ state.

The fixed-wavelength PES spectra have been deconvoluted with an iterative procedure [18], improving the effective resolution to about 15 meV as measured on the HeI-PES of 1,1-$C_2H_2Cl_2$.

In the fixed-wavelength PES, the photoelectron energy scale has been calibrated by recording the PES of a rare gas X-1,1-$C_2H_2Cl_2$ mixture (X = Ar, Kr and Xe), giving ±2 meV accuracy for the energy scale.

The Ar absorption spectrum between the $^2P_{3/2}$ and the $^2P_{1/2}$ ionization thresholds has been used to calibrate the 3m-NIM monochromator, with an accuracy better than 2 meV.

Energy steps of about 10 meV have been chosen for recording the TPES between 9 and 24 eV photon energy. The uncertainty on the energy position of a feature is estimated to be 6 meV. Between 10 and 20 eV, the TPES is recorded with an energy increment of 4 meV leading to an uncertainty for the energy positions of the order of 3 meV. These estimations are confirmed by the reproducibility of energy positions in different spectra over several measurement sessions.

3. Experimental results

3.1. HeI-, NeI- and ArII/ArI-PES

The deconvoluted HeI-PES of 1,1-$C_2H_2Cl_2$ as measured between 9.5 and 21 eV is shown in figure 1(a). A recording of the 9.5–13.0 eV range is shown in figure 1(b) with 4 meV increments. Electronic states and vibrational assignments discussed below are included.

Seven well-defined bands and presumably nine electronic states are observed between 9.5 and 21 eV. Their adiabatic and vertical ionization energies are listed in table 1 together with previously reported results obtained with HeI and HeII.

Table 1. Adiabatic and vertical ionization energies (eV) measured by HeI-, NeI- ArII-PES and by TPES using synchrotron radiation in this work and in previous reports [2–6].

This work							
HeI[a]		NeI[b]		ArII[c]		TPES[d]	
IE_{ad}	IE_{vert}	IE_{ad}	IE_{vert}	IE_{ad}	IE_{vert}	IE_{ad}	IE_{vert}
9.828	9.992	9.823	9.993	9.826	10.001	9.828	9.990
11.520	11.647	11.517	11.620	11.509	11.642	11.521	11.696
12.157	12.157	—	12.181	12.147	12.174	12.167	12.200
12.497	12.536	—	12.529	12.481	12.519	12.495	12.535
13.521	13.633	13.540	13.935		—	13.570	13.650
—	14.195	—	14.189			—	~14.1
15.539	—	15.620	—			15.620	15.820
18.496	18.496					~17.9	18.506

Previous reports									
[6]		[3]		[4]		[2]		[5]	
TPES		HeI		HeI		HeI		HeII	
IE_{ad}	IE_{vert}	IE_{ad}	IE_{vert}	IE_{ad}	IE_{vert}	IE_{ad}	IE_{vert}	IE_{ad}	IE_{vert}
	9.89	9.83	10.00		10.00	9.74	10.00	9.83	10.00
	11.68	11.46	11.67		11.62	11.38	11.66		11.7
	12.22	12.06	12.17		12.19	12.24			12.2
	12.55		12.51		12.48	12.5	12.55		12.5
	13.91		~13.7		~13.89	13.47	13.84		~13.8
	14.19		14.24		14.16		14.25		14.3
	16.15		16.27		16.2	15.49	15.89	15.4	16.8
	18.49		18.47		18.5		~18.42		18.5

[a] Uncertainty ±0.005 eV, see section 2.2.
[b] Uncertainty ±0.004 eV, see section 2.2.
[c] Uncertainty ±0.003 eV, see section 2.2.
[d] Uncertainty ±0.003 eV, see section 2.2.

The NeI-PES of 1,1-$C_2H_2Cl_2$ is shown in figure 2(a) between 9.5 and 16.8 eV. The HeI-PES is reproduced in the same energy range for comparison. Figure 2(b) displays the 9.5–13.0 eV energy range on an expanded scale. In both parts of the figure, several structures are marked by an asterisk to indicate the probable contribution of the NeI-16.67 eV resonance line. On comparing with the HeI-PES, differences are obvious and will be discussed in section 5. The results on the ionization energies are listed in table 1.

The ArI/ArII-PES of 1,1-$C_2H_2Cl_2$ is represented in figure 3. Asterisks mark the probable contributions of the ArI-11.828 eV line. In the same figure the HeI-PES is reproduced, normalized to the intensity of the first vibrational structure in the first band. This comparison clearly shows dramatic differences over the whole ionization energy range.

3.2. Threshold-PES

The TPES spectrum of 1,1-$C_2H_2Cl_2$ has been recorded between 9.5 and 30 eV with a pass energy $E_0 = 5$ V. Owing to the low transmission of the grating above 24 eV, an unfavorable signal/noise ratio is observed in this range of the spectrum. A well resolved spectrum between 9.5 and 20 eV, recorded at a pass energy $E_0 = 1$ V and with 5 meV energy increments, is shown in figure 4. For comparison, the same figure also displays the HeI-PES normalized to the intensity of the adiabatic transition in the first PES band. Table 1 lists the vertical ionization energies inferred from the TPES together with those from the HeI-, NeI- and ArII-PES.

Large differences between the HeI-PES and the TPES are observed. Compared to the intensity of the $\tilde{X}\,^2B_1$-band at 9.826 eV, the relative intensities of the PES-bands corresponding to the ionic excited states are considerably enhanced by the resonant photoionization process governing the TPES. The very long vibrational progression in the $\tilde{X}^2B_1$ band displays several intensity maxima at 9.99, 10.72, 11.06, 11.25 and 11.35 eV. As already pointed out earlier in the case of 1,1-$C_2H_2F_2$ [1] and 1,1-C_2H_2FCl [1], the HeI-PES intensity is more or less evenly distributed among the ground and the excited states of the ion, whereas the excited states dominate the TPES between 11.5 and 21 eV. The difference in the shape of the bands at about 14 eV and at 18.5 eV is also noteworthy. In the former, several maxima are observed between 13.6 and 15.2 eV. For the latter band, the signal

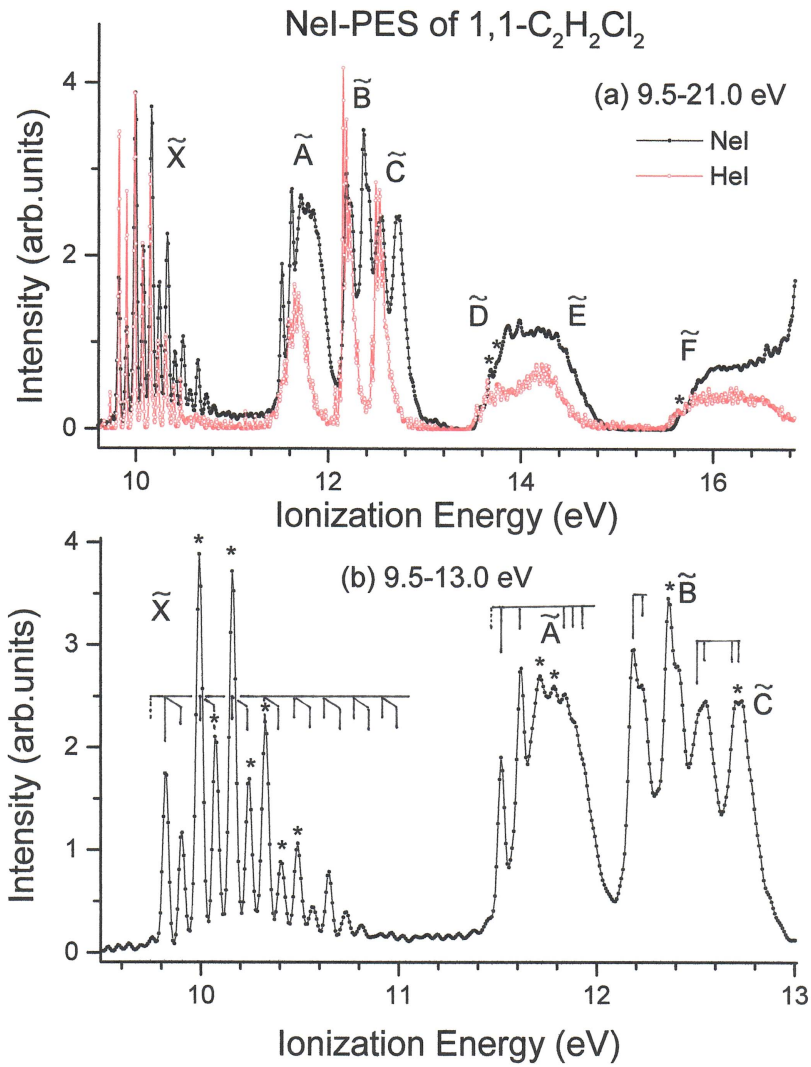

Figure 2. NeI- photoelectron spectrum (PES) of 1,1-$C_2H_2Cl_2$ between (a) 9.5 and 17 eV, and (b) 9.5 and 13.0 eV. Vertical bars show the vibrational structure. Only the two highest wavenumbers are represented for the $\tilde{X}^2B_1$ state.

increases very sharply at threshold (18.496 eV) in the HeI-PES and is narrow, whereas it rises up smoothly from 18.05 eV in the TPES and is much broader.

3.3. The CIS spectra

The CIS spectra have been recorded for the first eight electronic states of 1, 1-$C_2H_2Cl_2^+$. These are displayed in figure 5(a) together with the TPES. To facilitate the interpretation and discussion, the Δ-plot of the vacuum UV PAS of 1,1-$C_2H_2Cl_2$ has been reproduced in figure 5(b) [8] between 9.8 and 20 eV.

Owing to the wide extent of the vibrational population of the ground electronic state of 1, 1-$C_2H_2Cl_2^+$ observed in the TPES, a sequence of vibrationally resolved CIS spectra has been recorded between 9.83 and 20.0 eV. The result is shown in figure 6. The corresponding TPES spectrum is included in this figure. In this case too, marked differences of the spectral shape are noteworthy.

As mentioned in section 2.1, CIS spectra extending over large energy ranges are contaminated by Xe autoionization resonances at about 7.5 eV above threshold, due to the normalization procedure.

4. *Ab initio* calculations: methods and results

4.1. Computational tools

All calculations were performed using the Gaussian 09 software [19] with an aug-c.c.-pVDZ basis set [20] containing polarization and diffuse functions.

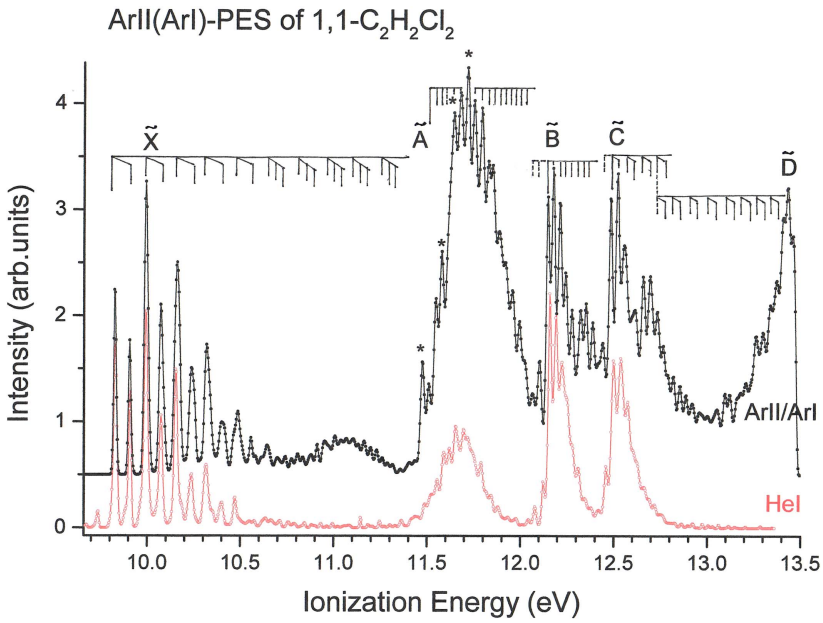

Figure 3. ArII/ArI- photoelectron spectrum (PES) of 1,1-$C_2H_2Cl_2$ between 9.5 and 13.5 eV. Vertical bars show the vibrational structure. Only the first and third levels of ν_5 of $\tilde{X}^2B_1$ state are represented to avoid overcrowding.

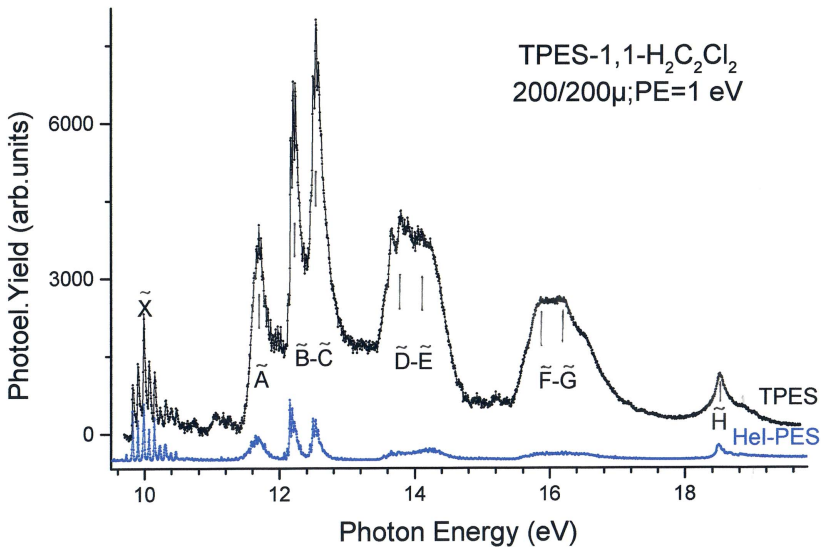

Figure 4. Threshold photoelectron spectrum (TPES) of 1,1-$C_2H_2Cl_2$ between 9.5 and 21 eV. The HeI photoelectron spectrum (PES) of 1,1-$C_2H_2Cl_2$ is reproduced for comparison. Vertical bars locate the vertical ionization energies.

The geometry optimizations have been performed at the CCSD(FC) [21, 22], B3LYP [23, 24], M06-2X [25] and TD-DFT(M06-2X) [26] levels. The CCSD(FC) level may be considered as the most accurate. The M06-2X is recognized as a very good new functional.

The molecular orbital (MO) configuration of 1,1-$C_2H_2Cl_2$ in the C_{2v} symmetry group is described by

$$1s(Cl1)^2,\ 1s(Cl2)^2,\ 1s(C1)^2,\ 1s(C2)^2,\ 2s(Cl1)^2,\ 2s(Cl2)^2,\ 2p_{x,y,z}(Cl1)^6,\ 2p_{x,y,z}(Cl2)^6$$
$$(1a_1)^2(1b_2)^2(2a_1)^2(3a_1)^2(2b_2)^2(4a_1)^2(1b_1)^2(3b_2)^2(5a_1)^2(1a_2)^2(4b_2)^2(2b_1)^2:\ \tilde{X}^1A_1,$$

where $1a_1$ is the first outer-valence shell orbital.

The wavenumbers characterizing the twelve vibrational normal modes were determined at the M06-2X, B3LYP and TDDF/M06-2X levels.

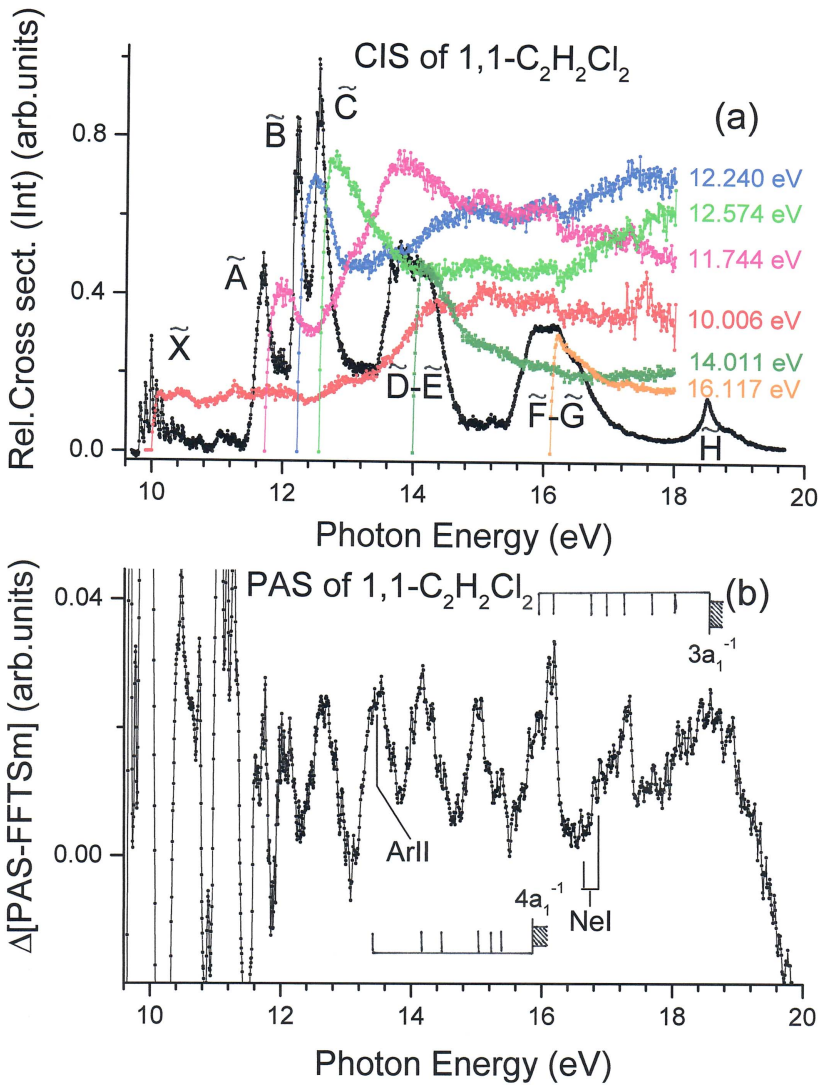

Figure 5. (a) CIS spectra of the first eight ionic states of 1,1 -$C_2H_2Cl_2^+$ between onset and 18 eV. The TPES spectrum is shown as a reference. (b) Δ-plot of the vacuum UV PAS of 1,1-$C_2H_2Cl_2$ in the same energy range [8].

4.2. Results of the calculations

The result of the geometry optimization of the neutral $\tilde{X}^1A_1$ ground state, of the cationic ground state, $\tilde{X}^2B_1$, and of several excited states are presented in table S1 which is available online at stacks.iop.org/JPCO/1/055030/mmedia (supplementary data), according to the atomic numbering shown in the same table, at three or four different calculation levels.

The vibrational normal modes for the different electronic states of the cation 1,1 -$C_2H_2Cl_2^+$ are represented in figure S1 (see supplementary data). The corresponding wavenumbers are listed in table 2. The present theoretical results can only be compared to those obtained by Zhou *et al* [7] and Takeshita [27]. This latter author reported on the *ab initio* calculated photoelectron spectrum of the three dichloroethylene isomers [27].

The vertical and adiabatic ionization energies calculated at several levels are presented in table 3. The contour maps of the involved MO, calculated at the RHF level for the neutral molecule optimized at the CCSF(FC) level, are represented in figure S2 (supplementary data).

5. Discussion

5.1. HeI-, NeI- and ArII/ArI-PES of 1,1-$C_2H_2Cl_2$ (figures 1–3)

The PES of 1,1-$C_2H_2Cl_2$ strongly varies with the energy of the exciting light source. As shown in figures 1–3 the extent of vibrational excitation involved with the three light sources is quite different. The relative intensities between the successive bands and within each band are altered. Owing to the numerous structures observed, each band as produced by the three excitation sources will be analyzed separately.

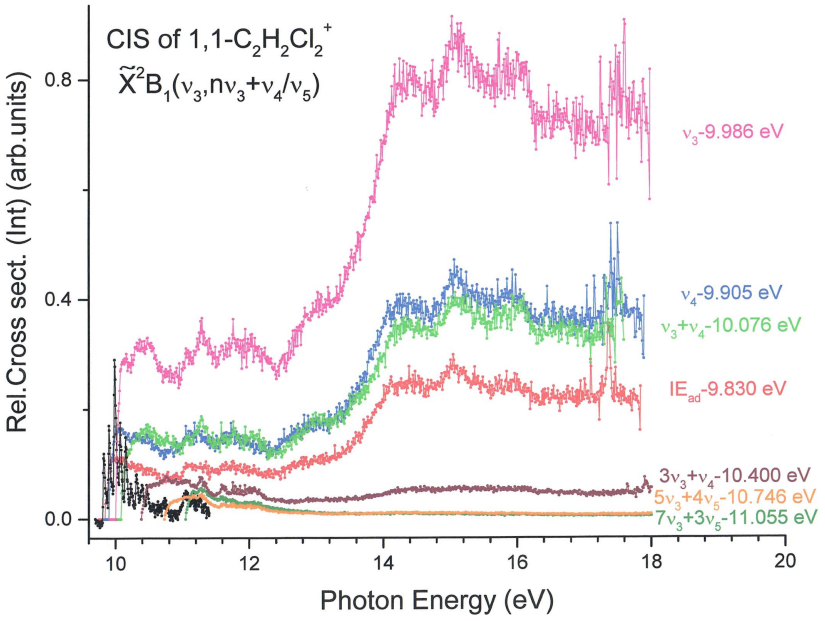

Figure 6. Vibrationally resolved CIS spectra for specific vibrations observed in the $\tilde{X}^2B_1$ state of 1,1 -$C_2H_2Cl_2^+$.

5.1.1. The $\tilde{X}^2B_1$- PES band (figures 1(b), 2(b) and 3)

The $\tilde{X}^2B_1$ band of 1, 1-$C_2H_2Cl_2^+$ excited by the HeI resonance line is observed between 9.7 and 10.5 eV (bold line in column 1 of table 4). Using the NeI- and ArII-resonance lines the cationic ground state is observed up to 11.076 ± 0.006 eV (levels in brackets in table 4) and 11.383 ± 0.004 eV (levels in square brackets in table 4) respectively.

The adiabatic ionization energy averaged over the results of five HeI- measurements and two NeI- and ArII-spectra is equal to $IE_{ad}(\tilde{X}^2B_1\text{-}1,\ 1\text{-}C_2H_2Cl_2^+) = 9.826 \pm 0.002$ eV, where the indicated error is the largest deviation from the average between all the measurements. A weak signal is observed at 9.746 ± 0.010 eV. It represents 8.6% of the intensity of the adiabatic transition and is assigned to a hot band involving $\omega_4 = 603\ cm^{-1}$ (0.075 eV) of the neutral 1,1-$C_2H_2Cl_2$ molecule [28], for which a contribution of 5.5% is predicted at room temperature, based on the Boltzmann distribution law.

As shown in table 1 this value of IE_{ad} is in good agreement with most previously reported results [2–5], ranging from 9.74 to 9.83 eV. The published value of 10.00 eV [2–5] corresponds to the $IE_{vert} = 9.992 \pm 0.001$ eV as measured in the present work. The calculated values listed in table 3 are in very good agreement with those reported in earlier and in the present work (see table 1).

The energy positions of the structures observed in the first PES band are listed in table 4. Considering only the results obtained by the HeI resonance line the transition energies and assignments are listed in columns 1 and 3. The strongest vibrational transitions correspond to an average spacing of 0.163 ± 0.006 eV (1320 ± 50 cm^{-1}). It is assigned to the C=C stretching vibrational normal mode involving ν_3 of a_1 symmetry (see figure S1). This assignment is consistent with the characteristics of the ionized $2b_1$ MO (with π character) (see figure S2). This value is in good agreement with previous determinations, i.e. 1290 cm^{-1} [4], 1320 cm^{-1} [3] or 0.16 eV (1290 cm^{-1}) [2]. Surprisingly, this vibration has not been observed by infrared spectroscopy of 1, 1-$C_2H_2Cl_2^+$ trapped in a solid Argon matrix [7]. In previous quantum chemical calculations, the harmonic wavenumber of 1366.1 cm^{-1} and the anharmonic value of 1340.6 cm^{-1} were predicted [7]. In the present work, the calculated wavenumbers that can be related to a C=C stretching are equal to $\omega_2 = 1499\ (1477)\ cm^{-1}$ and $\omega_3 = 1364\ (1330)\ cm^{-1}$ at the M06-2X (B3LYP) level (see table 2). Takeshita [27] calculated $\omega_2 = 1592\ cm^{-1}$ and $\omega_3 = 1435\ cm^{-1}$. The second predicted value (ω_3) is obviously in better agreement with the experimental results.

However, integrating the HeI-PES data in the list of results obtained with NeI and ArII, a lowering of the spacing is observed and ascribed to anharmonicity. The data analysis leads to $\omega = 1347 \pm 8\ cm^{-1}$ (0.167 ± 0.001 eV) and $\omega x = 3.9 \pm 1.1\ cm^{-1}$ (0.48 ± 0.14 meV). This wavenumber is in good agreement with the predicted anharmonic value [7].

The further analysis of the first PES band reveals a more complex structure with at least two other vibrational spacings. The strongest of these transitions is characterized by $\omega = 653 \pm 24\ cm^{-1}$ (0.081 ± 0.003 eV) in very good agreement with 650 cm^{-1} reported by Lake and Thompson [3] by HeI-PES and 642.8 cm^{-1} measured by infrared spectroscopy [7]. Other HeI-PES determinations were reported i.e., 560 cm^{-1} [4] and 730 cm^{-1} [2].

Table 2. Wavenumbers (cm^{-1}) of the vibrational normal modes of 1,1-$C_2H_2Cl_2$ in its ground state and of 1,1 -$C_2H_2Cl_2^+$ in its ground and excited states, calculated at the indicated levels.

Symmetry	$\tilde{X}^1A_1$	$\tilde{X}^2B_1$	$\tilde{A}^2B_2$	$\tilde{B}^2A_2$	$\tilde{C}^2A_1$
			M06-2X [TD-DFT]// B3LYP		
a_1					
ν_1	3184//3175	3185//3148	3162 [3165] //3153	3169 [3167] //3161	3171 [3177] //3169
ν_2	1702//1665	1499//1477	1748 [1676] //1706	1699 [1670] //1671	1529 [1621] //1524
ν_3	1388//1390	1364//1330	1372 [1370] //1378	1382 [1382] //1388	1415 [1398] //1411
ν_4	624//595	672//642	639 [640] //604	584 [582] //570	547 [621] //520
ν_5	299//296	327//322	287 [259] //261	281 [277] //279	308 [247] //305
a_2					
ν_6	690//686	356 //354	686 [717] //689	688 [682] //689	665 [698] //676
b_1					
ν_7	925//905	983//979	971 [1038] //960	987 [1035] //982	972 [1045] //966
ν_8	460//468	486 //475	371 [341] //379	386 [352] //395	423 [361] //427
b_2					
ν_9	3292//3279	3314//3275	3268 [3273] //3257	3276 [3279] //3266	3289 [3293] //3276
ν_{10}	1095//1086	1196//1153	986 [974] //984	977 [971] //984	*1508 [1010]* //919
ν_{11}	794//765	903//871	679 [711] //642	494 [399] //553	*787 [493]* //518
ν_{12}	378//377	364//364	317 [314] //326	367 [311] //370	404 [403] //i352
	$\tilde{D}^2B_2$	$\tilde{E}^2B_1$	$\tilde{F}^2A_1$	$\tilde{G}^2B_2$ (TS)	$\tilde{H}^2A_1$ (TS)
			TD-DFT		
a_1					
ν_1	2877	3151	2774	2900	3057
ν_2	1660	1644	1598	1785	1767
ν_3	1196	1383	1127	1439	1418
ν_4	647	510	561	500	592
ν_5	317	254	263	212	291
a_2					
ν_6	737	713	625	*i991*	233
b_1					
ν_7	611	962	875	1819	705
ν_8	513	368	365	403	*i701*
b_2					
ν_9	2901	3272	3696	2841	3405
ν_{10}	2220	1243	1781	1000	1159
ν_{11}	620	836	894	451	841
ν_{12}	416	355	380	223	376

Table 3. Vertical and adiabatic ionization energies (eV) determined at four calculation levels for the cationic states resulting from direct ionization. Previous quantum chemical calculation results reported by Parkes *et al* [6] are included.

State	$\tilde{X}^2B_1$		$\tilde{A}^2B_2$		$\tilde{B}^2A_2$		$\tilde{C}^2A_1$	
Level	IE_{vert}	IE_{ad}	IE_{vert}	IE_{ad}	IE_{vert}	IE_{ad}	IE_{vert}	IE_{ad}
CCSD	9.89	9.62	11.60	11.24	12.13	12.07	12.51	12.44
M06-2X	9.99	9.70	11.68	11.32	12.19	12.13	12.52	12.44
B3LYP	9.81	9.58	11.33	11.07	11.76	11.71	12.10	12.03
TD-DFT[a]	9.99	9.70	11.68	11.39	12.28	12.24	12.50	12.42
[6]	9.69	—	11.41	—	11.94	—	12.32	—

State	$\tilde{D}^2B_2$		$\tilde{E}^2B_1$		$\tilde{F}^2A_1$		$\tilde{G}^2B_2$		$\tilde{H}^2A_1$	
Level	IE_{vert}	IE_{ad}	IE_{vert}	IE_{ad}	IE_{vert}	IE_{ad}	IE_{vert}	IE_{ad}	IE_{vert}	IE_{ad}
TD-DFT[a]	13.82	13.3	14.32	14.03	15.86	15.34	16.37	16.04	18.78	18.62
[6]	13.89	—	14.20	—	15.95	—	16.58	—	18.93	—

[a] For the $\tilde{X}^2B_1$ state, there is no *IE* determination at the TD-DFT level and the reference energy for this state at this calculation level is taken equal to the DFT(M06-2X) *IE*.

This wavenumber is close to the predicted harmonic value of 681.8 cm^{-1} or anharmonic value of 672.4 cm^{-1} [7] and 682 cm^{-1} [27] for ν_4 (symmetric C–Cl stretching) of a_1 symmetry (see figure S1). In the neutral molecule this vibration is characterized by $\omega_4 = 603$ cm^{-1} [28]. The present work provides 624 (595) cm^{-1} for the neutral and 672 (642) cm^{-1} for the cation as calculated at the M06-2X (B3LYP) level (see table 2).

Finally, a third and very weak vibrational excitation, combined with the excitation of ν_3 and ν_4, is observed with $\omega = 470 \pm 20$ cm^{-1} (0.058 ± 0.003 eV). Surprisingly, it has mainly been observed so far only in the HeI-PES. Its intensity is rapidly decreasing as the excitation of ν_3 increases. It could not be observed in the fairly well resolved ArII-PES. The doublet structure of the excitation source likely prevents its observation in the NeI-PES. A first explanation would be the large difference in the population mechanism involved in the HeI-PES on the one hand, where direct ionization prevails, and in NeI- and ArII-PES on the other hand, where autoionization is expected to be involved. The latter two excitation lines are resonant with broad and fairly strong photoabsorption bands [8] of 1,1-$C_2H_2Cl_2$, displayed in figure 5(b). This wavenumber fits reasonably well with our calculated ν_8 wavenumber of 486 (475) cm^{-1} (see table 2), corresponding to an out-of-plane deformation of b_2 symmetry. This symmetry forbidden excitation is expected to be of very low intensity (see figure S1). A similar observation and assignment was proposed in the HeI-PES of 1,1-$C_2H_2F_2$ [30].

Combined with the excitation of the 1347 cm^{-1} normal mode, a fourth vibrational transition has to be invoked to assign three structures in the HeI-PES, i.e. at 10.179, 10.347 eV and at 10.488 eV. Extending our observations to the NeI- and ArII-PES, the combination of 1347 cm^{-1} with this vibration dominates these spectra. Figure 3 illustrates how far the $n\nu_3$ progression extends in combination with this vibrational motion. In the ArII-PES an additional sequence of structures is generated extending from 10.8 to 11.4 eV with a maximum at 11.06 eV. The associated spacing, averaged over all observed levels up to 11.383 eV, is $\omega = 274 \pm 16$ cm^{-1} (0.034 ± 0.002 eV). This wavenumber could correspond to the vibrational Cl–C–Cl scissor motion ν_5 (see figure S1) of a_1 symmetry which is predicted at 331.2 cm^{-1} in [7], at 346 cm^{-1} in [27] and at 327 (322) cm^{-1} in the present work. The corresponding transition has not been observed by infrared spectroscopy [7]. In the neutral molecule, this normal mode has a wavenumber of 299 cm^{-1} [28].

5.1.2. The $\tilde{A}^2B_2$-PES band (figures 1(b), 2(b) and 3)

The second HeI-PES band extending from 11.5 to 12.1 eV consists of a smooth and regular structure. In the NeI-PES, the relative intensity of several structures of the same band is strongly modified. Apart from ArI-PES contributions, the intensity distribution appears considerably enhanced in the ArII-PES as shown by the comparison with its HeI-PES (see figure 3). The average positions of the structures observed in these spectra are listed in table 5.

The lowest threshold is determined at $IE_{ad}(\tilde{A}^2B_2\text{-}1,\ 1\text{-}C_2H_2Cl_2^+) = 11.515 \pm 0.006$ eV whereas $IE_{vert} = 11.647 \pm 0.005$ eV. These results can be compared with those reported in previous works, i.e. 11.38 and 11.66 eV [2], 11.46 and 11.67 eV [3], or 11.62 eV [4] and 11.7 eV [5]. These values are in good agreement with our calculated M06-2X IE_{ad}(11.32 eV) and IE_{vert}(11.68 eV) values (table 3).

The transition observed at 11.47 ± 0.02 eV has very likely to be ascribed, at least partially, to a hot band transition. The wavenumber separation of 347 ± 60 cm^{-1} (0.043 ± 0.007 eV) is close to 299 cm^{-1} measured for ν_5 in the neutral molecule [28]. In the NeI-PES the intensity ratio between the two transitions measured at

Table 4. Transition energies (eV), assignments and average wavenumbers (cm^{-1}) inferred from the structures observed in the HeI-, NeI-, ArII-/ArI-PES and in the TPES of the $\tilde{X}^2B_1$ band of 1,1 -$C_2H_2Cl_2^+$. Conversion factor 1 eV = 8065.545 cm^{-1} [29]. Weak to very weak structures are mentioned in italics.

		Assignments	
PES[a] (HeI, NeI and ArII)	TPES[b]		Wave numbers of the normal modes
9.746 ± 0.010		HB (ν_4)	
9.826 ± 0.002	9.830	**IE$_{ad}$**($\tilde{X}^2B_1$)	ω_3 = 0.163 ± 0.006 eV
	9.865	ν_5	1322 ± 48 cm^{-1}
9.882 ± 0.005	*9.880*	ν_8	By B–S extrapolation[c]:
9.906 ± 0.004	9.905	ν_4	ω_3 = 0.167 ± 0.001 eV
	9.940	$\nu_4 + \nu_5$	1347 ± 8 cm^{-1}
9.968 ± 0.005	*9.960*	$\nu_4 + \nu_8$	ω_3x_3 = 3.9 ± 1.1 cm^{-1}
9.993 ± 0.001[d]	9.990	ν_3 (IE_{vert})	
	10.031	$\nu_3 + \nu_5$	ω_4 = 0.081 ± 0.003 eV
10.050 ± 0.005	*10.045*	$\nu_3 + \nu_8$	653 ± 24 cm^{-1}
10.072 ± 0.001[d]	10.076	$\nu_3 + \nu_4$	
	10.110	$\nu_3 + \nu_4 + \nu_5$	ω_8 = 0.058 ± 0.003 eV
	10.127	$\nu_3 + \nu_4 + \nu_8$	468 ± 40 cm^{-1}
10.157 ± 0.005[d]	10.155	$2\nu_3$	
10.179 ± 0.005	*10.186*	$2\nu_3 + \nu_5$	ω_5 = 0.034 ± 0.002 eV
10.239 ± 0.003[d]	10.235	$2\nu_3 + \nu_4$	274 ± 16 cm^{-1}
10.320 ± 0.005[d]	10.320	$3\nu_3$	In the TPES[c]:
10.347 ± 0.005		$3\nu_3 + \nu_5$	ω_5 = 0.037 ± 0.004 eV
	10.385	$3\nu_3 + 2\nu_5$	298 ± 32 cm^{-1}
10.405 ± 0.003[d]	*10.400*	$3\nu_3 + \nu_4$	
	10.440	$3\nu_3 + \nu_4 + \nu_5$	
10.472 ± 0.005[d]		$4\nu_3$	
10.488 ± 0.003	*10.480*	$4\nu_3 + \nu_5$	
(10.561 ± 0.004)[e]		$4\nu_3 + \nu_4$	
(10.643 ± 0.001)[e]		$5\nu_3$	
[10.698][f]		$5\nu_3 + \nu_5$	
(10.738 ± 0.003)[e]		$5\nu_3 + 3\nu_5$	
(10.772 ± 0.003)[e]	*10.75*	$5\nu_3 + 4\nu_5$	
(*10.810 ± 0.004*)[e]		$6\nu_3$	
[*10.835*][f]		$6\nu_3 + \nu_5$	
[*10.878*][f]	*10.87*	$6\nu_3 + 2\nu_5$	
(*10.911 ± 0.002*)[e]		$6\nu_3 + 3\nu_5$	
(*10.958 ± 0.006*)[e]		na	
[*10.972*][f]		$7\nu_3$	
(*11.012 ± 0.008*)[e]		$7\nu_3 + \nu_5$	
(*11.076 ± 0.006*)[e]	*11.06*	$7\nu_3 + 3\nu_5$	
[*11.105*][f]		$7\nu_3 + 4\nu_5$	
[*11.132*][f]		$8\nu_3$	
[*11.164*][f]	*11.17*	$8\nu_3 + \nu_5$	
[*11.199*][f]		$8\nu_3 + 2\nu_5$	
[*11.231*][f]		$8\nu_3 + 3\nu_5$	
[*11.262*][f]	*11.27*	$8\nu_3 + 4\nu_5$	
[*11.289*][f]		$9\nu_3$	
[*11.317*][f]		$9\nu_3 + \nu_5$	
[*11.383*][f]		$9\nu_3 + 3\nu_5$	

[a] Positions of structures averaged over the HeI-, NeI- and ArII-spectra are listed with their largest deviation from the average. The HeI band is observed up to 10.488 eV as marked by a bold line in this table.

[b] Uncertainty estimated to be ±0.003 eV.

[c] Average values over HeI-, NeI-, ArII-PES and TPES spectra. A second ω_3 and ω_5 value results from a Birge–Sponer (B–S) extrapolation and TPES measurements respectively (see figures 4 and 7).

[d] In the NeI spectrum, peaks at these positions contain contributions of the NeI-16.670 eV (134455.7 cm^{-1}) line and are shown by asterisks in figure 2(b).

[e] In brackets: positions of structures averaged over the NeI- and ArII-spectra listed with their largest deviation from the average.

[f] In square brackets: positions of the structures only observed in the ArII-spectrum recorded with an energy increment of 4 meV.

Table 5. Transition energies (eV), assignments and average wavenumbers (cm^{-1}) inferred from the structures observed in the HeI-, NeI-, ArII-/ArI-PES and in the TPES of the $\tilde{A}^2B_2$ band of 1,1 -$C_2H_2Cl_2^+$. Conversion factor 1 eV = 8065.545 cm^{-1} [29]. Weak to very weak structures are mentioned in italics.

		Assignments	
PES (HeI, NeI and ArII)	TPES[c]		Wave numbers of the normal modes
11.473 ± 0.017[a]	*11.485*	HB (ν_5)[a]	Average value in PES
11.515 ± 0.006	*11.521*	$IE_{ad}(0,0)$	$\omega_5 = 0.035 \pm 0.005$ eV
11.551 ± 0.005[a]	11.556	ν_5	282 ± 40 cm^{-1}
11.585 ± 0.006	11.581	$2\nu_5$	
11.619	11.621	$3\nu_5$	Average value in TPES
11.647 ± 0.005[a]	11.661	$IE_{vert}(4\nu_5)$	$\omega_5 = 0.035 \pm 0.004$ eV
11.687 ± 0.007[a]	11.696	$5\nu_5$	282 ± 32 cm^{-1}
11.717 ± 0.002[b]	11.726	$6\nu_5$	
11.747 ± 0.005[a,b]	11.756	$7\nu_5$	
11.789 ± 0.003	11.791	$8\nu_5$	
11.821 ± 0.006	11.826	$9\nu_5$	
11.845 ± 0.004	11.866	$10\nu_5$	
11.884 ± 0.004	11.901	$11\nu_5$	
11.927 ± 0.007	11.941	$12\nu_5$	
11.966 ± 0.010	11.976	$13\nu_5$	
11.997 ± 0.004	12.011	$14\nu_5$	
12.034 ± 0.012	12.051	$15\nu_5$	
12.072 ± 0.007	12.081	$16\nu_5$	

[a] Contributions of the $\tilde{X}^2B_1$ ($\nu_x = 0$ at 9.826 eV or 1 at 9.993 eV) state of 1, 1-$C_2H_2Cl_2^+$ as ionized by the 11.830 eV (95417.6 cm^{-1}) or 11.620 (93723.8 cm^{-1}) lines of ArI-shown by asterisks in figure 3.

[b] Contributions of the NeI-16.670 eV (134455.7 cm^{-1}) line in the NeI-PES shown by asterisks in figure 2.

[c] Uncertainty estimated to be ±0.003 eV.

11.464 and 11.517 eV is about 17%, close to the Boltzmann law prediction of 23%. In the ArII-PES the intensity observed at 11.477 eV is contaminated by the ionization to the $\tilde{X}^2B_2$ ground state with the ArI resonance line at 11.830 eV.

Table 5 reports the assignments of all the structures observed in this band. It shows that the whole band could be accounted for by one progression involving a single vibrational mode characterized by an average separation of 0.035 ± 0.005 eV (282 ± 40 cm^{-1}). Lake and Thompson [3] report a wavenumber of 270 cm^{-1}, perfectly compatible with the present determination. This progression is observed up to $v = 16$. It could be assigned to ν_5 which has been calculated at 287 (261) cm^{-1} at M06-2X (B3LYP) level in this work. Takeshita [27] predicted 320 cm^{-1} for the Cl–C–Cl scissoring mode. From the shape of the ionized $4b_2$ MO (see figure S2) and the results of the optimized geometry (see table S1), the Cl–C–Cl scissor mode should be an important component of the excited mode confirming the assignment of the progression to ν_5 (see figure S1).

5.1.3. The $\tilde{B}^2A_2$- and $\tilde{C}^2A_1$-PES bands (figures 1(b), 2(b) and 3)

The third and fourth bands of the HeI-PES are well separated. Both contain well-resolved regular structures. Compared to the HeI-PES, the NeI- and ArII-spectra show noticeable modifications of these bands (see figures 2(b) and 3). Furthermore, in the NeI-PES these two bands are contaminated by the contribution of the NeI-16.670 eV resonance line (marked by asterisks in figure 2(b)). In contrast, the ArII-PES of these two bands cannot be perturbed by ArI- lines at 11.62–11.83 eV.

HeI-ionization to the third band provides unambiguously $IE_{ad} = IE_{vert} = 12.152 \pm 0.005$ eV. This should correspond to the $\tilde{B}^2A_2$ state of 1,1 -$C_2H_2Cl_2^+$. Two lower-lying structures are observed at 12.122 ± 0.004 eV and 12.079 ± 0.004 eV. Their relative intensity with respect to the adiabatic transition is 20% and 9% respectively whereas the predicted value of the Boltzmann population for one and two quanta of $\omega \approx 300$ cm^{-1} (0.037 eV) vibration is 24% and 6% respectively. This suggests assigning these two transitions to hot bands from $v = 1$ and $v = 2$ of the ν_5 vibration of the neutral 1,1-$C_2H_2Cl_2$ ground state (see table 2). The present IE_{ad} measurement can be compared with previously reported values at 12.16 eV [2], 12.17 eV [3], 12.19 eV [4] and 12.2 eV [5] by HeII-PES. Our calculated M06-2X values for IE_{ad} and IE_{vert} are respectively equal to 12.13 and 12.19 eV (see table 3).

In the HeI-PE spectrum the intensity of the features observed in the third band steeply decreases upon increasing energy. The average energy positions and their assignment are listed in table 6. The progression

Table 6. Transition energies (eV), assignments and average wavenumbers (cm^{-1}) as deduced from the structures observed in the HeI-, NeI-, ArII-/ArI-PES and in the TPES of the $\tilde{B}^2A_2$ and $\tilde{C}^2A_1$ bands of 1,1 -$C_2H_2Cl_2^+$. Conversion factor 1 eV = 8065.545 cm^{-1} [29]. Weak to very weak structures are mentioned in italics.

PES			Assignments	
ArII/HeI	NeI	TPES[a]		Wave number of the normal modes
12.079 ± 0.004			HB($\nu_5 = 2$)	$\tilde{B}^2A_2$ Averaged value:
12.122 ± 0.004		12.135	HB($\nu_5 = 1$)	In PES:
12.152 ± 0.005		12.167	$IE_{ad}(0,0)$	$\omega_5 = 0.033 \pm 0.004$ eV
12.185 ± 0.009[b]	12.185	12.200[b]	ν_5	266 ± 32 cm^{-1}
12.217 ± 0.005	12.228	12.230	$2\nu_5$	In TPES:
12.244 ± 0.003		12.260	$3\nu_5$	$\omega_5 = 0.032 \pm 0.002$ eV
12.277 ± 0.003		12.290	$4\nu_5$	258 ± 16 cm^{-1}
12.316 ± 0.007		12.320	$5\nu_5$	
12.347 ± 0.004[b]	12.363[c]	12.355	$6\nu_5$	
12.383 ± 0.003		12.390	$7\nu_5$	
				$\tilde{C}^2A_1$
12.458 ± 0.005		12.460	HB	
12.488 ± 0.007		12.495	$IE_{ad}(0,0)$	
12.536 ± 0.006[b]	12.529	12.535[b]	ν_5	
12.575 ± 0.005	12.552	12.572	ν_4	
12.610 ± 0.005		12.615	$\nu_4 + \nu_5$	
12.656 ± 0.005		12.650	$2\nu_4$	
[12.695][d]	12.702		$2\nu_4 + \nu_5$	
[12.735][b,d]	12.734[c]		$3\nu_4$	
[12.766][d]			$3\nu_4 + \nu_5$	
[12.789][d]			$3\nu_4 + 2\nu_5$	
[12.821][d]			$4\nu_4$	$\omega_4 = 0.066 \pm 0.005$ eV
[12.854][d]			$4\nu_4 + \nu_5$	530 ± 40 cm^{-1}
[12.887][d]			$4\nu_4 + 2\nu_5$	$\omega_5 = 0.032 \pm 0.006$ eV
[12.919][d]			$5\nu_4$	260 ± 50 cm^{-1}
[12.958][d]			$5\nu_4 + \nu_5$	
[13.001][d]			$6\nu_4$	
[13.052][d]			$6\nu_4 + 2\nu_5$	
[13.095][d]			$7\nu_4$	
[13.122][d]			$7\nu_4 + \nu_5$	
[13.181][d]			$8\nu_4$	
[13.208][d]			$8\nu_4 + \nu_5$	
[13.263][d]			$9\nu_4$	
[13.299][d]			$9\nu_4 + \nu_5$	
[13.338][d]			$10\nu_4$	
[13.373][d]			$10\nu_4 + \nu_5$	
[13.408][d]			$11\nu_4$	
[13.432][d]			$11\nu_4 + \nu_5$	

[a] Uncertainty estimated to be ±0.003 eV.

[b] Energy position of the vertical ionization energies IE_{vert} in the ArII- and TPES spectra.

[c] Energy position of the ionization induced by the NeI-line at 16.670 eV as shown by asterisks in figure 2.

[d] In square brackets: structures observed in the ArII-PES spectrum only. The uncertainty is estimated to be ±0.003 eV.

involves a single vibrational normal mode with $\omega = 258 \pm 16$ cm^{-1} (0.032 ± 0.002 eV). This value has to be compared with the only measurement reported by Lake and Thompson [3] of 270 cm^{-1}. Furthermore, it has to be stressed that in the NeI- and ArII-PES (i) $IE_{ad} = IE_{vert}$ no longer holds and $IE_{vert} = 12.181 \pm 0.005$ eV and 12.174 ± 0.003 eV respectively, and (ii) a second intensity maximum is observed at 12.347 eV or 12.363 eV, respectively. Such changes of the intensity profile have already been observed earlier when autoionization is involved [18, 31] (see also section 5.1.1). The wavenumber of 258 cm^{-1} is close to that measured for ν_5 in the neutral molecule, i.e. 299 cm^{-1} [28]. The shape of the ionized $1a_2$ MO (see figure S2), the results of the geometry optimization, and the M06-2X (B3LYP) calculated wavenumber value of 281 (279) cm^{-1} validate the assignment of ν_5 to the progression (Cl–C–Cl scissoring in figure S1). Previously Takeshita's quantum chemical calculation [27] led to $\omega_5 = 308$ cm^{-1}.

HeI-PES leads to $IE_{ad} = IE_{vert} = 12.488 \pm 0.007$ eV for the fourth band. The structure lying at 12.458 ± 0.005 eV is ascribed to a hot band transition from $v = 1$ of ν_5 of the neutral molecule. This band is

assigned to the $\tilde{C}^2A_1$ state of 1, 1-$C_2H_2Cl_2^+$. The intensity of the vibrational structure of this band decreases regularly up to 12.656 eV for HeI-, 12.734 eV for NeI- and 13.432 eV for ArII-PES. As for the third band, the IE_{vert} is blue shifted in the latter two spectra: at 12.536 ± 0.006 eV in NeI- and ArII-PES. The IE_{ad} in the HeI-PES can be compared with previous determinations at 12.50 eV [2], 12.51 eV [3], 12.48 eV [4] and 12.5 eV [5] by HeII-PES. Our calculated M06-2X values for IE_{ad} and IE_{vert} are 12.44 and 12.52 eV respectively (see table 3).

The ArII-PE spectrum displays a well resolved vibrational progression up to 13.432 eV as shown in figure 3 and table 6. The intensity nearly vanishes above 12.919 eV and rises up again to 13.432 eV. From 13.1 to 13.5 eV, the intensity of the vibrational structure is affected by the strong zero-energy (ZEKE) electron signal.

Considering all data available and, in particular, the ArII-PES over the whole 12.488–13.432 eV energy range, the vibrational structure could be accounted for by two vibrational modes, ν_4 and ν_5, as reported in table 6 and shown in figure 3. These data can be fitted assuming quadratic and cubic anharmonic corrections, leading to $\omega_4 = 530 \pm 40$ cm^{-1} (0.066 ± 0.005 eV), $\omega_4 x_4 = -33 \pm 9$ cm^{-1}, and $\omega_4 y_4 = -1.9 \pm 0.5$ cm^{-1}. These results, in particular the relatively strong negative quadratic anharmonic contribution, might be linked to a strong perturbation in the potential energy hypersurface of the $\tilde{C}^2A_1$ state of 1, 1-$C_2H_2Cl_2^+$, which is close in energy to the $\tilde{B}^2A_2$ state. It is interesting to note here a similarity with our previous PES data on 1,1-$C_2H_2F_2$ [1]. The main vibrational progression associated with the $\tilde{E}^2A_1$ state of 1, 1-$C_2H_2F_2^+$ also displays a strong quadratic anharmonicity ($\omega x = -54 \pm 14$ cm^{-1}) and a smaller cubic anharmonicity ($\omega y = -6.5 \pm 1.2$ cm^{-1}).

The value found for ω_4 is in the range predicted by our quantum chemical calculations (see table 2), that is, between 520 and 620 cm^{-1}. Furthermore, the ν_4 vibrational excitation is combined with the excitation of the ν_5 mode with $\omega_5 = 260 \pm 30$ cm^{-1} (0.032 ± 0.004 eV). The latter assignment is based on the satisfactory agreement with our theoretical predictions, in the 250–300 cm^{-1} range. These assignments are compatible with the characteristics of the $5a_1$ MO depicted in figure S2 and with the normal modes described in figure S1.

5.1.4. The $\tilde{D}^2B_2$-$\tilde{E}^2B_1$ and $\tilde{F}^2A_1$-$\tilde{G}^2B_2$-PES bands (figure 1)

The fifth and sixth PES-bands are broad and spread over 1.0–1.5 eV. They both involve two overlapping electronic states likely consisting of a dense vibrational structure. This structure is difficult to disentangle owing to overlapping progressions.

A closer examination of the fifth PE-band allows us to measure the $IE_{ad} = 13.521 \pm 0.004$ eV for the fifth electronic state and assign it to the $\tilde{D}^2B_2$ state of 1, 1-$C_2H_2Cl_2^+$. An $IE_{vert} = 13.633$ eV is also measured and could be compared to the literature values 13.84 [2], ~13.7 eV [3] and 13.8 eV by HeII-PES [5]. The calculated TD-DFT *IE* values are respectively 13.30 eV and 13.82 eV, which are compatible with the experimental data (see table 3 and figure S2).

In the same way, but less reliable, $IE_{ad} = 14.05$ or 14.09 eV and $IE_{vert} = 14.19$ or 14.24 eV could be proposed for the fifth electronic state. These *IE*'s are assigned to the $\tilde{E}^2B_1$ state of 1, 1-$C_2H_2Cl_2^+$. TD-DFT calculations predict *IE* values at 14.03 and 14.32 eV in good agreement with the observed values (see table 3 and figure S2). In the literature 14.25 eV [2], 14.24 eV [3], 14.16 eV [4] and 14.3 eV [5] have been reported.

For the first component of the sixth PE-band $IE_{ad} = 15.539 \pm 0.003$ eV is measured and $IE_{vert} \approx 15.9$ eV is estimated. The corresponding TD-DFT *IE* predictions for the ionization to the $\tilde{F}^2A_1$ state of 1,1 -$C_2H_2Cl_2^+$ are 15.34 eV and 15.86 eV respectively, in satisfactory agreement with the observed values (see table 3 and figure S2). These values can be compared to 15.49 eV [2] and 15.4 eV [5] for IE_{ad} and to 15.89 eV [2], 16.20 eV [3], 16.27 eV [4] and 16.8 eV [5] for IE_{vert}. These three latter values likely correspond to the IE_{ad} of the second component of this PE-band. The calculated IE_{ad} and IE_{vert} for the $\tilde{G}^2B_2$ ionic state of 1,1-$C_2H_2Cl_2$ are respectively 16.04 eV and 16.37 eV (see table 3 and figure S2). For this state, only the maximum could be determined at 16.16 eV.

5.1.5. The $\tilde{H}^2A_1$-PES band (figure 1)

The seventh and last band observed in the HeI-PES lies at $IE_{ad} = 18.496 \pm 0.003$ eV which has to correspond to the ninth adiabatic ionization of 1,1-$C_2H_2Cl_2$ in its $\tilde{H}^2A_1$ electronic state. The (0, 0) transition dominates the spectrum. This result can be compared with previous IE_{ad} determinations by HeI- and HeII-PES, i.e. at ~18.42 eV [2], 18.47 eV [3], 18.50 eV [4] and 18.5 eV [5]. Parkes *et al* [6] report $IE_{vert} = 18.49$ eV. The quantum chemical calculations in the present work predict $IE_{ad} = 18.62$ eV and $IE_{vert} = 18.78$ eV.

Only the few first structures could be analyzed up to 18.8 eV. The intensity is steeply decreasing and a fairly short likely anharmonic progression is observed with $\omega = 621 \pm 8$ cm^{-1} (0.077 ± 0.001 eV). This progression is combined with a low energy vibration characterized by $\omega = 194 \pm 24$ cm^{-1} (0.024 ± 0.006 eV). Only Lake and Thompson reported an analysis of the vibrational structure and mentioned a wavenumber of 1290 cm^{-1}. This value is about twice the value proposed in the present work.

Our quantum chemical calculations (table S1) suggest that the ionization from the $3a_1$ MO would lead to the vibrational excitation of the C–H and C=C stretching modes and also of the H–C–H and Cl–C–Cl bending modes (see figures S1 and S2). Comparing the experimental results with the predicted wavenumbers listed in table 2, the most satisfactory assignment is $\omega_4 = 621 \pm 8$ cm^{-1} and $\omega_5 = 194 \pm 24$ cm^{-1}.

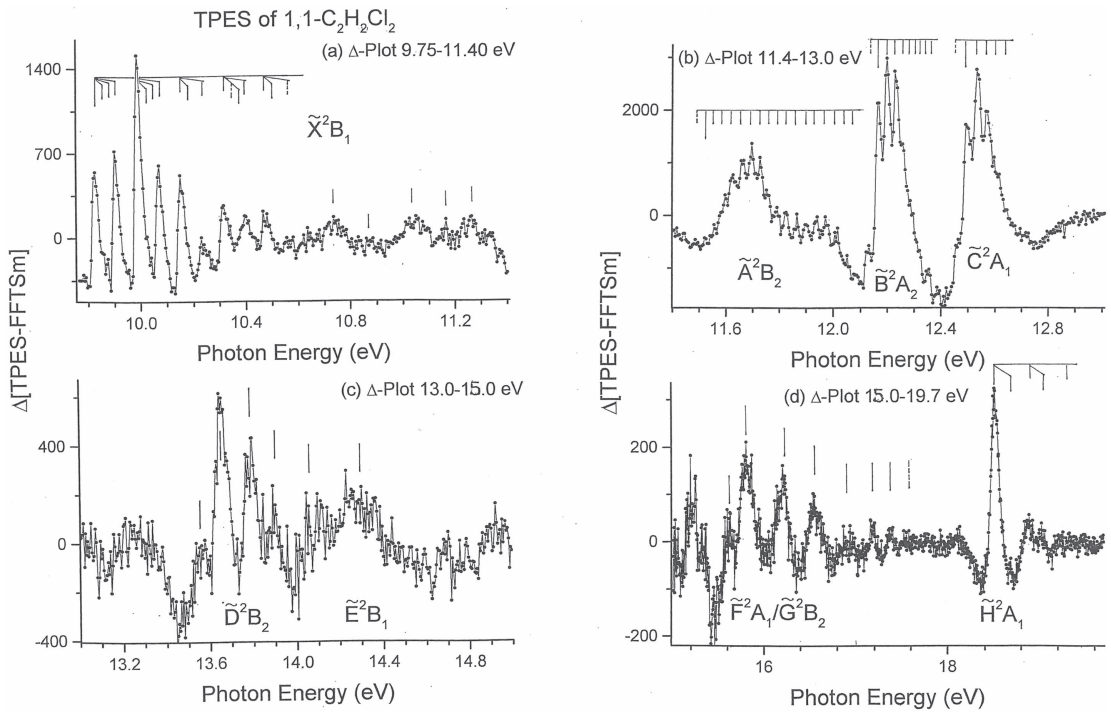

Figure 7. Δ-plot of the TPE spectrum in the (a) 9.75–11.4 eV, (b) 11.4–13 eV, (c) 13–15 eV and (d) 15–19.7 eV photon energy regions. Vertical bars indicate vibrational structure.

5.2. Threshold PES of 1,1-$C_2H_2Cl_2$ (figures 4 and 7)

The ionization and excitation mode are markedly different in the TPES and in the fixed wavelength PES. To record a TPES, the molecular system is resonantly excited by continuously scanning the vacuum UV light energy. The usefulness of this technique is that besides the successive ionic states, also the neutral states interacting with the ionization continuum through resonant autoionization and producing low-energy electrons, are involved. The Franck–Condon zones associated with these intermediate transitions may strongly differ from those involved in the direct ionization process usually governing HeI-PES, thus giving rise to a quite different PES.

The TPES observed in this work is reproduced in figure 4 between 9.5 and 20 eV and is compared to the HeI-PES normalized to the adiabatic transition for the ionic ground state. Major differences between the two spectra are obvious. The most visible aspect is the large increase in the relative intensity of almost all TPES bands. The successive adiabatic and/or vertical ionization energies are listed in table 1. To enhance the vibrational structure of the successive TPES bands, the subtraction method has been applied (see section 2.2). The resulting Δ-plot is shown on an expanded ionization energy scale in figures 7(a)–(d).

The energy position of the features observed in the $\tilde{X}^2B_2$-TPES band is listed in table 4. For most of the structures the agreement with the fixed-wavelength PES data is satisfactory. It has to be pointed out that the intensity at 10.990 eV is noticeably higher than in the HeI-PES (see also the NeI-PES in figure 2). However, in the 9.830–10.480 eV energy range, the TPES shows (and confirms) the excitation of the ν_5 vibrational mode at 9.865, 9.940, 10.110 and 10.385 eV successively. These features are not observed in the low-energy region of the first HeI-PES band, contrary to the more favorable situation in the better resolved TPES. The average energy separation is 0.037 ± 0.004 eV in the TPES whereas this value is 0.034 ± 0.002 eV as deduced from the HeI-PES (see column 4 in table 4).

As shown in figures 4 and 7(a) the ground ionic state is populated well above 10.480 eV. The signal/noise ratio in the Δ-plot is quite low. However, several maxima are observed and listed in table 4 and are compared with observations in NeI- and ArII-PES. Also in these cases the agreement is satisfactory.

The Δ-plot corresponding to the $\tilde{A}^2B_2$, the $\tilde{B}^2A_2$ and the $\tilde{C}^2A_1$ TPES bands is displayed in figure 7(b). They clearly reveal the associated vibrational structure which is listed in tables 5 and 6.

For the broad and abundantly structured $\tilde{A}^2B_2$ TPES band the shape is very close to the fixed wavelength PES. Only its relative intensity is considerably enhanced in the TPES. The average separation energy of 0.035 ± 0.004 eV for the single vibrational progression involved in this ionic state is in very good agreement with the value of 0.035 ± 0.005 eV deduced from the fixed wavelength PES.

Similarly to the large enhancement of the intensity of the $\tilde{A}^2B_2$ TPES band, the $\tilde{B}^2A_2$ and the $\tilde{C}^2A_1$ TPES bands are the strongest in the TPES. Here also, the features observed in these bands confirm those detected by HeI- and ArII-PES. The energy positions are listed in table 6.

Owing to the fairly low signal/noise ratio in the Δ-plot only approximate energy values could be measured for the features observed between 13.5 and 15 eV (see figure 7(c)). Additional abundant unresolved autoionization structures seem to bring about a significant contribution. For the $\tilde{E}^2B_2$ band only an intensity maximum could be estimated at about 14.25 eV. It seems that, in this energy region, autoionization strongly perturbs the regular progression which was observed by HeI-PES. The energy range of 13.5–17.3 eV corresponds to several broad absorption bands of 1,1-$C_2H_2Cl_2$, with strong to weak intensities [8] (see figure 5(b)).

The Δ-plot of the energy range covered by the three last TPES bands is represented in figure 7(d). Also in these cases only fairly broad but well resolved features are observed. Between 16.1 and 17.6 eV several features are observed at 15.82, 16.21, 16.56, 16.9, 17.2, 17.4 and 17.6 eV. This fairly surprising regular pattern might be related to the oscillation of the Franck–Condon factors governing the autoionizing transitions from the neutral excited states to the final $\tilde{F}^2A_1$ and $\tilde{G}^2B_2$ ionic states. The vibrational structure is likely hidden in the noise on the successive maxima. Similar effects have been observed and investigated in NeI-PES of diatomic molecules [31].

The last ionic $\tilde{H}^2A_1$ state is observed at $IE = 18.506 \pm 0.003$ eV which can be compared with the adiabatic $IE = 18.496 \pm 0.003$ eV measured by HeI-PES (see section 5.1.5 and table 1). As already pointed out earlier and clearly observed in figure 4, the base of the peak at 18.5 eV is strongly broadened towards lower energy, i.e. to about 17.9 eV. In the Δ-plot of this energy range (see figure 7(d)) a maximum is observed near 18.13 eV. Above 18.5 eV this plot reveals peaks at 18.68 eV, 18.86 eV, 19.04 eV and 19.22 eV successively. Two intervals could be recognized: one of about 0.35 eV and another of about 0.16–0.17 eV.

As drawn in figure 7(d), these structures could be assigned to two major vibrations, i.e. $h c\omega \approx 0.36$ eV (2900 cm^{-1}) and $h c\omega \approx 0.17$ eV (1370 cm^{-1}). A closer examination of the major peak at 18.5 eV reveals several shoulders with intervals of 0.025–0.035 eV (200–280 cm^{-1}). These can be compared with the value of 0.024 ± 0.006 eV inferred from the HeI-PES. The only vibrational analysis of this band in the He-I PES is that of Lake and Thompson [3], who reported a wavenumber of 1290 cm^{-1}. Their interpretation differs however from that of the present work (see section 5.1.5). Comparing the TPES results with the quantum chemical predictions, the ν_1 ($\omega_1 = 2900$ cm^{-1}), ν_3 ($\omega_3 = 1370$ cm^{-1}) and likely ν_5 ($\omega_5 = 200$–280 cm^{-1}) are excited. The first two vibrations have not been observed in the present HeI-PES. Again, resonant autoionization is suspected to strongly perturb the branching among the photoionization and, as a consequence, the vibrational band profile.

5.3. CIS spectra of 1,1-$C_2H_2Cl_2$ (figures 5 and 6)

The individual CIS spectra related to the first eight electronic states have been recorded over a range of about 10 eV photon energy (figure 5(a)). In the case of the $\tilde{D}^2B_2$, $\tilde{E}^2B_1$, $\tilde{F}^2A_1$ and $\tilde{G}^2B_2$ TPES bands the CIS spectra have been recorded for the energy corresponding to the maximum of the band.

The difference between the CIS spectral profiles below and above 14 eV photon energy is noteworthy. Below 14.0 eV, the CIS spectra show a complex shape and a strong cross-section variation. Above 14.0 eV, a mainly monotonic behavior is observed. This observation might be related to a large difference in the population mechanism of the ionic states below and above 14 eV.

Above 14 eV, we may infer from the shape of the CIS spectra that the population of the $\tilde{D}\ ^2B_2$-$\tilde{E}^2B_1$ and $\tilde{F}\ ^2A_1$-$\tilde{G}^2B_2$ states has to occur resonantly or nearly resonantly through the autoionization of highly excited (Rydberg) states of the neutral molecule. For clarity of this discussion, the Δ-plot of the vacuum UV PAS of 1,1-$C_2H_2Cl_2$ is reproduced in figure 5(b) [8]. From 14 eV upward, several Rydberg states were identified, e.g., at 14.15 eV/14.31 eV[$(4a_1^{-1})3d/4s$] and 16.15 eV/16.91 eV [$(3a_1^{-1})3p/3d$] [8].

Below 14 eV, the CIS spectra related to the $\tilde{A}^2B_2$, $\tilde{B}^2A_2$ and $\tilde{C}^2A_1$ ionic states show a quite similar profile: a 'resonant' maximum near the onset followed by an increase of the cross-section modulated by several structures. The maximum near the onset in the CIS($\tilde{A}$) and CIS($\tilde{B}$) spectra correspond to Rydberg states at about 12.06 eV [$(5a_1^{-1})6p/8p$] and 12.5 eV [$(5a_1^{-1}8p\sigma)$] [8]. Both converge to the $\tilde{C}^2A_1$ ionic state. Several shoulders and maxima are observed, which correlate with PAS bands. A sudden decrease of the cross-section is observed at 16.1 eV in the CIS spectra of $\tilde{X}^2B_1$, $\tilde{A}^2B_2$, $\tilde{B}^2A_2$ and $\tilde{C}^2A_1$ states. This may be correlated to the onset of the $\tilde{F}^2A_1$-$\tilde{G}^2B_2$ channel at 16.117 eV. It may also be related to the resonance observed at 16.1 eV in the PAS. This resonance shows an asymmetric profile in the absorption spectrum [8], which might be interpreted as a Fano profile. The decrease of the state-resolved ionization cross sections (CIS spectra) at this energy is compatible with a partial population transfer from the continuum to the discrete state, a situation linked to the interference between the continuum and Rydberg wave functions and which is expected to give rise to Fano profiles.

Figure 5(a) shows a typical CIS spectrum obtained for the $\tilde{X}^2B_1$ state. Figure 6 displays a set of seven CIS spectra recorded for well defined (as indicated in the figure) vibrational levels of the ground state of the

Table 7. Maxima or band limits (eV) observed (x) or missing (o) in the CIS spectra of the specified vibrations of the ground state $\tilde{X}^2B_2$ of 1,1 -$C_2H_2Cl_2^+$. The assignments refer to the corresponding transitions in the vacuum UV PAS of 1,1-$C_2H_2Cl_2$ [8].

CIS Max.	10.4	11.1	11.3	11.5–12.4	12.4–13.9	13.9–14.7	15.1	16.1–16.3
IE_{ad}	x	x	o	o	x	x	x	x
ν_4	x	x	x	x	x	x	x	x
ν_3	x	x	x	x	x	x	x	x
$\nu_3 + \nu_4$	x	x	x	x	x	x	x	x
$3\nu_3 + \nu_4$	o	o	x	x	x	x	x	x
$5\nu_3 + 4\nu_5$	—	o	o	x	o	o	o	o
$7\nu_3 + 3\nu_5$	—	o	o	x	o	o	o	o
Assignm. [8]	$4b_2 \rightarrow 4p\sigma$	$1a_2 \rightarrow 4p\sigma$	$3b_2 \rightarrow 3p\sigma$	$1a_2 \rightarrow$ nd, $n = 5, 6, 7, 9$ $5a_1 \rightarrow 6p, 8p$	$5a_1 \rightarrow 8p\sigma$ $4a_1 \rightarrow 3p$	$4a_1 \rightarrow 4$ s, 3d	$4a_1 \rightarrow 5p$	$3a_1 \rightarrow 3p$

molecular ion. Also in this narrow energy range the CIS spectral profiles for different vibrational levels show marked differences with respect to the structure and intensity. These observations are summarized in table 7.

The CIS spectrum of IE_{ad} at 9.830 eV shows a nearly constant cross section up to 12.5 eV. Above this energy it increases as do the CIS spectra recorded at 9.905, 9.986, 10.076 and 10.400 eV which all show the same autoionizing contributions. These are identified in the vacuum UV PAS [8] and shown in table 7. In the HeI-PES these vibrations are all populated by direct Franck–Condon transition from the neutral ground state of the molecule. In contrast, the CIS spectra at 10.746 and 11.055 eV are related to vibrational states populated only through autoionization processes in the NeI- and ArII-PES and in the TPES. At 1.0–1.5 eV above onset, these cross-sections decrease regularly to reach the baseline at about 16 eV. A bold line in table 7 separates the two types of vibrational states.

6. Conclusions

A detailed photoelectron spectroscopic investigation of 1,1-$C_2H_2Cl_2$ up to 22 eV has been performed including constant wavelength HeI-, NeI-, and ArII/ArI-PES, as well as the variable wavelength TPES and CIS spectra for all accessible ionic electronic states and for selected vibrational states of the ground ionic electronic state. Seven electronic bands have been identified in this photon energy range. These bands were assigned with reference to quantum chemical calculations. The first four bands show an extended vibrational structure. For each of these bands, vibrational wavenumbers are inferred and compared to quantum chemical predictions. The very good correlation between the theoretical predictions and the experimental values allowed us to assign the normal modes. These vibrational data are also compared to previous investigations. The structures observed in the CIS spectra of the successive electronic states of the molecular ion below 14 eV exhibit strong correlation with those observed in the vacuum UV PAS of 1,1-$C_2H_2Cl_2$. Vibrationally resolved CIS spectra recorded for the $\tilde{X}^2B_1$ state of 1, 1-$C_2H_2Cl_2^+$ show a similar behavior only for those vibrations which are populated by direct Franck–Condon transitions from the neutral ground state of the molecule. The additional vibrational levels which appear in the NeI and ArII PES involve, however, autoionization transitions.

Acknowledgments

This work has been financially supported by the University of Liège and by the European Community which provided access to the BESSY large-scale synchrotron facility. DD thanks the Belgian Science Policy (IAP no P6/19), supported by the Belgian program on Interuniversity Attraction Poles.

ORCID iDs

R Locht https://orcid.org/0000-0002-9175-2720

References

[1] Locht R, Jochims H-W and Leyh B 2012 *Chem. Phys.* **405** 124
Locht R, Dehareng D and Leyh B 2012 *J. Phys. B: At. Mol. Opt. Phys.* **45** 115101
Locht R, Dehareng D and Leyh B 2014 *Mol. Phys.* **112** 1520
Locht R, Dehareng D and Leyh B 2014 *J. Phys. B: At. Mol. Opt. Phys.* **47** 85101
Locht R, Dehareng D and Leyh B 2014 *J. Phys. B: At. Mol. Opt. Phys.* **47** 175101

[2] Jonathan N, Ross K and Tomlinson V 1970 *Int. J. Mass Spectrom. Ion Phys.* **4** 51
[3] Lake R F and Thompson H 1970 *Proc. R. Soc.* A **315** 323
[4] Wittel K and Bock H 1974 *Chem. Ber.* **107** 317
[5] Von Niessen W, Åsbrink L and Bieri G 1982 *J. Electron Spectrosc. Relat. Phenom.* **26** 173
[6] Parkes M A, Ali S, Howle C R, Tuckett R P and Malins A E R 2007 *Mol. Phys.* **105** 907
[7] Zhou H, Gong Y and Zhou M 2007 *J. Phys. Chem.* A **111** 603
[8] Locht R, Dehareng D and Leyh B 2017 *J. Phys. Commun.* **1** 045013
[9] Servais C and Locht R 1995 *Chem. Phys. Lett.* **236** 96
[10] Locht R, Leyh B, Hottmann K and Baumgärtel H 1997 *Chem. Phys.* **220** 217
[11] Lindau I, Helmer J C and Uebbing J 1973 *Rev. Sci. Instrum.* **44** 265
[12] Codling K and Madden R P 1976 *J. Res. Natl Bur. Stand.* **76A** 1
[13] Carbonneau R, Bolduc E and Marmet P 1973 *Can. J. Phys.* **51** 505
[14] Carbonneau R and Marmet P 1973 *Can. J. Phys.* **51** 2202
Carbonneau R and Marmet P 1974 *Phys. Rev.* A **9** 1898
[15] Locht R, Leyh B, Denzer W, Hagenow G and Baumgärtel H 1991 *Chem. Phys.* **155** 407
[16] Locht R, Leyh B, Dehareng D, Hottmann H and Baumgärtel H 2010 *J. Phys. B: At. Mol. Opt. Phys.* **43** 015102
[17] Palmer M H, Ridley T, Jones N C, Goreno M, de Simone M, Grazioli C, Zhang T, Biczysko M, Baiardi A and Peterson K A 2016 *J. Chem. Phys.* **144** 204305
Palmer M H, Ridley T, Jones N C, Goreno M, de Simone M, Grazioli C, Zhang T, Biczysko M, Baiardi A and Peterson K A 2016 *J. Chem. Phys.* **144** 124302
Palmer M H, Ridley T, Jones N C, Goreno M, de Simone M, Grazioli C, Zhang T, Biczysko M, Baiardi A and Peterson K A 2015 *J. Chem. Phys.* **143** 164303
[18] Locht R, Caprace G and Momigny J 1984 *Chem. Phys. Lett.* **111** 560
[19] Frisch M J *et al* 2009 *Gaussian 09* (Wallingford CT: Gaussian, Inc.) Revision A.02
[20] Dunning T H Jr 1989 *J. Chem. Phys.* **90** 1007
[21] Cizek J 2007 On the use of the cluster expansion and the technique of diagrams in calculations of correlation effects in atoms and molecules *Advances in Chemical Physics* ed R LeFebvre and C Moser 14 (New York: Wiley) pp 35–89
[22] Scuzeria G E and Schaefer III H F 1989 *J. Chem. Phys.* **90** 3700
[23] Parr R G and Yang W 1989 *Density Functional Theory of Atoms and Molecules* (New York: Oxford University Press)
[24] Becke A D 1993 *J. Chem. Phys.* **98** 5648
[25] Zhao Y and Truhlar D G 2008 *Theor. Chem. Acc.* **120** 215
[26] Van Caillie C and Amos R D 2000 *Chem. Phys. Lett.* **317** 159
[27] Takeshita K 1999 *J. Chem. Phys.* **110** 6792
[28] Shimanouchi T 1972 *Tables of Molecular Vibrational Frequencies* (*NSRDS-NBS 39*) Consolidated vol 1 (Washington, DC: The Government Printing Office)
[29] Mohr P J, Taylor B N and Newell D B 2016 *J. Phys. Chem. Ref. Data* **45** 043102
Mohr P J, Newell D B and Taylor B N 2016 *Rev. Mod. Phys.* **88** 035009
[30] Harvey J, Hemberger P, Bödi A and Tuckett R P 2013 *J. Chem. Phys.* **138** 124301
[31] Natalis P, Pennetreau P, Longton L and Collin J E 1982 *Chem. Phys.* **73** 191
Natalis P 1973 *Mém. Cl. Sc. Acad. R. Belg.* **XLI** 61